Short title: *SELF-PRUNING* regulates auxin responses in tomato

Corresponding author details:

Agustin Zsögön

Universidade Federal de Viçosa, Brazil

Phone: +55 31 3899 2592

Fax: +55 31 3899 4139

agustin.zsogon@ufv.br

Title: *SELF-PRUNING* affects auxin responses synergistically with the cyclophilin A DIAGEOTROPICA in tomato

Authors: Willian B. Silva[1a], Mateus H. Vicente[2a], Jessenia M. Robledo[1a], Diego S. Reartes[2], Renata C. Ferrari[4], Ricardo Bianchetti[4], Wagner L. Araújo[3], Luciano Freschi[4], Lázaro E. P. Peres[2], Agustin Zsögön[1]*

Affiliations

[1]*Departamento de Biologia Vegetal, Universidade Federal de Viçosa, CEP 36570-900, Viçosa, MG, Brazil*

[2]*Laboratory of Hormonal Control of Plant Development. Departamento de Ciências Biológicas, Escola Superior de Agricultura "Luiz de Queiroz", Universidade de São Paulo, CP 09, 13418-900, Piracicaba, SP, Brazil*

[3]*Max-Planck Partner group at the Departamento de Biologia Vegetal, Universidade Federal de Viçosa, 36570-900, Viçosa, MG, Brazil.*

[4]*Instituto de Biociências, Universidade de São Paulo, CEP 05508-900, São Paulo, SP, Brazil*

[a]These authors contributed equally

WBS, williambatistadasilva@gmail.com

MHV, mhvicente21@gmail.com

JMR, kjmoncaleano@gmail.com

DSR, diego.reartes@gmail.com

RCF, renata.callefe@gmail.com

RB, bianchetti.ricardo@gmail.com

WLA, wlaraujo@ufv.br

LF, freschi@usp.br

LEPP, lazaro.peres@usp.br

Summary: The antiflorigenic signal SELF-PRUNING, which controls growth habit, exerts its effects through auxin transport, signaling and metabolism in tomato.

Author contributions

WBS, MHV and JMR generated the plant material and conducted experiments. WBS, MHV, JMR, DSR, LF, RCF and RB conducted experiments and prepared figures and/or tables. LF and WLA designed experiments, contributed reagents/materials/analysis tools and reviewed drafts of the paper. AZ and LEPP conceived and designed the experiments, analyzed the data and wrote the paper.

Corresponding author: AZ, agustin.zsogon@ufv.br

Abstract

The *SELF PRUNING* (*SP*) gene is a key regulator of growth habit in tomato (*Solanum lycopersicum*). It is an ortholog of *TERMINAL FLOWER 1*, a phosphatidyl-ethanolamine binding protein with anti-florigenic activity in *Arabidopsis thaliana*. A spontaneous loss-of-function *sp* mutation has been bred into a large number of industrial tomato cultivars, as it produces a suite of pleiotropic effects that are favorable for mechanical harvesting, including determinate growth habit, short plant stature and simultaneous fruit ripening. However, the physiological basis for these phenotypic differences has not been thoroughly explained. Here, we show that the *sp* mutation alters polar auxin transport as well as auxin responses such gravitropic curvature and elongation of excised hypocotyl segments. We further demonstrate that free auxin levels and auxin-regulated gene expression patterns are altered in *sp*, with epistatic effects of *diageotropica*,

a mutation in a cyclophilin A protein-encoding gene. Our results indicate that SP impacts growth habit in tomato, at least in part, via changes in auxin transport and responsiveness. These findings hint at novel targets that could be manipulated in the control of growth habit and productivity.

Key words: growth habit, *Solanum lycopersicum*, polar auxin transport, development, plant architecture

Introduction

Shoot architecture is a key agricultural trait determined mainly by side branching, internode elongation and shoot determinacy (Wang and Li, 2008). Each of these parameters configures an active research area where considerable theoretical and applied knowledge has been gained over the last decade. Shoot determinacy is a domestication trait in crop species as diverse as soybean (*Glycine max*), common bean (*Phaseolus vulgaris*) and tomato (*Solanum lycopersicum*) (Pnueli et al., 1998; Tian et al., 2010; Repinski et al., 2012). Tomato is a perennial species cultivated as annual. Wild tomatoes display indeterminate growth, resulting from a sequential addition of modules (sympodial units) formed by three leaves and an inflorescence. Sympodial growth starts in tomato when the vegetative apical meristem is converted into floral after a series of 8-12 internodes with leaves (Samach and Lotan, 2007). Vegetative growth, however, continues through the top-most axillary meristem, which grows vigorously displacing the inflorescence to the side and producing a new sympodial unit with three leaves and an inflorescence. This process is indefinitely iterated by concatenation of sympodial units one on top of the other. A spontaneous recessive mutant with compact, bushy growth habit and a reduced number of leaves in successive sympodial units was discovered in 1914 (Yeager, 1927; MacArthur, 1934). It was later shown that the mutation is a single nucleotide substitution in the *SELF-PRUNING* (*SP*) gene (Pnueli et al., 1998), which shares sequence similarity with a group of mammalian polypeptides involved in cell signaling, phosphatidylethanolamine binding proteins (PEBPs) (Hengst et al., 2001; Kroslak et al., 2001). Breeding of this mutation into industrial tomato cultivars was instrumental in the advent of mechanical harvest (Rick, 1978; Stevens and Rick, 1986). The loss-of-function *sp* mutant leads to determinate growth habit, as opposed to the indeterminate growth habit of wild-type tomatoes. The determinate

growth habit occurs via progressively reduced number of leaves per sympodium until termination in two consecutive inflorescences that top vertical growth of the plant (Samach and Lotan, 2007). Hence, this phenotype leads to simultaneous fruit ripening, therefore allowing mechanical harvest in field-grown processing tomatoes (Stevens and Rick, 1986).

SP belongs to the *CETS* gene family, which comprises *CENTRORADIALIS* (*CEN*) and *TERMINAL FLOWER 1* (*TFL1*) of *Antirrhinum* and *Arabidopsis*, respectively (Wickland and Hanzawa, 2015). *SINGLE FLOWER TRUSS (SFT)*/*SP3D* – a homolog of *FLOWERING LOCUS T* (*FT*) and *HEADING DATE 3A* (*HD3A*) in Arabidopsis and rice, respectively – is another *CETS* gene involved in the control of growth habit in tomato (Alvarez et al., 1992; Kojima et al., 2002). Unlike *sp* mutants, which do not affect flowering time, tomato *sft* loss-of-function mutants are late flowering, and also show a disruption in sympodial growth pattern: they produce a single and highly vegetative inflorescence, alternating solitary flowers and leaves (Molinero-Rosales et al., 2004). The final phenotypic outcome produced by SP and SFT depends on their local ratio, with the former maintaining meristems in an indeterminate state and the latter promoting the transition to flowering (Park et al., 2014). Heterozygous *sft* mutants in a homozygous *sp* mutant background display yield heterosis in tomato (Krieger et al., 2010). Hence, the *SP*/*SFT* genetic module has been proposed as a target to increase crop yield via changes in plant architecture (McGarry and Ayre, 2012; Zsögön et al., 2017). It has also been previously suggested that *SP* function could be linked to auxin (Pnueli *et al.*, 2001), a hormone with strong effects on plant morphogenesis (Berleth and Sachs, 2001).

Auxin is a key controller of plant development; however, its role in the regulation of plant growth habit is still unclear. An aspect that sets auxin apart from other plant hormones is the relatively well understood nature of its transport through the plant body (Friml, 2003; Petrášek and Friml, 2009). Polar auxin transport (PAT), which occurs basipetally from the apical meristem, is critically important for the distribution of auxin within plant tissues (Rubery and Sheldrake, 1974; Sheldrake, 1974). PAT works as an organizer of apical-basal polarity in the plant body (Friml et al., 2006), thus controlling a multiplicity of developmental processes (Reinhardt et al., 2003; Blilou et al., 2005; Scarpella et al., 2006).

It has recently been shown that the cyclophilin A protein DIAGEOTROPICA (DGT) affects polar auxin transport (PAT) in tomato (Ivanchenko et al., 2015). DGT is a cyclophilin A protein with peptidyl-prolyl trans-cis isomerase (PPIase) enzymatic activity (Takahashi et al., 1989; Oh et al., 2006). Cyclophilins catalyse not only rate-limiting steps in the protein folding pathway but can also participate in the folding process as molecular chaperones (Kumari et al., 2013). DGT function is highly conserved across plant taxa (Lavy et al., 2012). In tomato, some of the most significant phenotypic defects caused by the lack of functional DGT protein are horizontal shoot growth, thin stems, altered secondary vascular differentiation and roots lacking lateral branches (Zobel, 1973; Muday et al., 1995; Coenen et al., 2003). Here, we investigated whether *SP* affects auxin responses, by itself, and in combination with *DGT*. We produced four combinations of functional and loss-of-function mutant alleles of *SP* and *DGT* (*i.e. SP DGT*, *SP dgt*, *sp DGT* and *sp dgt*) in a single tomato genetic background (cv. Micro-Tom) and assessed a series of physiological responses to auxin. We found that free auxin levels, polar auxin transport and gravitropic curvature of the shoot apex are all altered by *SP*. Our results further show that *SP* and *DGT* reciprocally affect *AUX/IAA* and *ARF* transcript abundances at the sympodial meristem, the key niche of *SP* function in growth habit.

Results

Comparison of the four combinations of homozygous wild-type and mutant lines for *SP* and *DGT* (*i.e.*, *SP DGT*, *SP dgt*, *sp DGT* and *sp dgt*), showed that growth habit was affected solely by *SP* and not by *DGT* (Fig. 1). Regardless of their *DGT* or *dgt* allele, *SP* plants showed indeterminate growth whereas *sp* mutants were always determinate (Fig. 1). Time to flowering, however, was affected by both genes in combinatorial fashion. *dgt* plants flowered late, independently of the *SP* allele (Fig. 1). The *sp DGT* genotype showed consistently precocious flowering, and this was confirmed in an independent experiment by analysis of the rate of shoot apical meristem maturation (Fig S1). The number of leaves to the first inflorescence was also affected by the combination of alleles (Fig. 1), albeit not reflecting the time to flowering. The *dgt* mutant produced more leaves before flowering, but this effect was abolished in the double mutant *sp dgt*. Regardless of their *SP* allele, *dgt*

mutants exhibited markedly reduced transcript abundance of the flowering inducer *SINGLE FLOWER TRUSS* (*SFT*) compared to *DGT* plants (Fig. 1), which fits with the delayed flowering in these mutants in both *SP* and *sp* backgrounds (Fig. 1).

The tomato cultivar Micro-Tom (MT) harbors a mutation in *DWARF* (*D*), a gene coding for a key enzyme in the brassinosteroid biosynthesis pathway (Bishop et al., 1999). Since brassinosteroids are known to influence the flowering induction network (Domagalska et al., 2010; Li et al., 2010), we ascertained whether *D* could be influencing the effects of *SP* on flowering time. Using a near-isogenic MT line harboring the functional *D* allele (Carvalho et al., 2011), we constructed four allelic combinations of *SP* and *D* (*i.e. SP D*, *SP d*, *sp D* and *sp d*, Fig S2) and assessed their flowering time. The results show an effect of *D* on flowering time (Fig. S2) but not on the number of leaves produced to the first inflorescence, which was again reduced exclusively by the presence of the *sp* mutant allele (Fig. S2). Axillary branching was affected mainly by the *SP* gene, which led to reduced bud outgrowth in plants carrying the wild-type allele; the *dgt* mutation, however, exacerbated this repressing effect (Fig. 1). *sp* mutants, on the other hand, branched more profusely when combined with *dgt* than *DGT* (Fig. 1). Thus, *dgt* can enhance apical dominance or increase branching, depending on the presence or absence of a functional *SP* allele, respectively. The number of leaves on the primary shoot was increased by *SP*, regardless of the *DGT* allele (Table 1). Plant height was additively controlled by both genes, whereas no difference between genotypes was found in the length of the fourth internode or leaf insertion angle (Table 1). Stem diameter was increased by functional *DGT*, irrespective of the *SP* allele (Table 1). The number of inflorescences was synergistically determined by both genes, whereby pairing of functional *SP* and *DGT* led to an increased number compared to all other allele combinations (Table 1).

Next, the endogenous levels of free indolyl-3-acetic acid (IAA), which is the most abundant auxin in plants (Bartel and Fink, 1995), was determined in three sections of tomato seedlings: leaves plus cotyledons, hypocotyls and roots (Fig. 2). In leaves plus cotyledons, IAA concentration was more than twice higher in *sp dgt* double mutant than in the other three genotypes (Fig. 2). In the hypocotyl tissues, *SP DGT* seedlings had the lowest free IAA content, the *sp* and *dgt* single mutants presented intermediate values and

the double mutant (*sp dgt*) exhibited the highest IAA levels (Fig. 2). Although root IAA levels were clearly higher than in the other hypocotyl regions analyzed, no statistically significant differences in root IAA content was observed between the four genotypes (Fig. 2).

To understand the variation in endogenous free IAA levels within the seedling tissues and among the four genotypes, we next quantified polar auxin transport (PAT) in hypocotyl segments. PAT was highest in *SP DGT*, intermediate in *sp* and *dgt* single mutants, and lowest in the double mutant (Fig. 3). This indicates that both *sp* and *dgt* alleles reduce PAT and that their effects were additive. As PAT and auxin concentration are known to influence vascular patterning (Scarpella, 2017), we also analyzed xylem anatomy in cross-sections of stems in adult plants (Fig 3). Quantification of xylem vessel density and mean vessel size revealed an antagonistic relationship between *SP* and *DGT*. Whereas *SP* tends to reduce vessel density and increase their size, *DGT* increases vessel density with concomitantly lower vessel sizes (Fig. 3). These results, however, obscure a more complex pattern, which is revealed when analyzing the vessel size distributions. The functional *DGT* allele increased the incidence of larger (>800 μm^2 cross-sectional area) vessels, particularly in *sp* mutant plants (Fig 3). Another physiological response affected by PAT is negative gravitropism of the shoot (Morita, 2010). The kinetics of gravitropic curvature in seedling shoots was affected by both *SP* and *DGT* (Fig. 4). Loss of *SP* function decreased gravitropic response in both *DGT* and *dgt* backgrounds. Hypocotyl elongation in response to exogenous auxin and *in vitro* rhizogenesis from cotyledon explants are assays to determine auxin sensitivity (Cary et al., 2001). The *dgt* mutation considerably reduces hypocotyl responsivity to auxin in all concentrations, as described previously (Kelly and Bradford, 1986; Rice and Lomax, 2000). The functional *SP* allele increased hypocotyl elongation in a *DGT* background and also exerts a significant compensatory effect on the elongation response in the *dgt* mutant (Fig. 4). In the *in vitro* root regeneration assay, as expected, root formation was reduced in *dgt* mutants (Coenen and Lomax, 1998), but also in *sp* compared to *SP* in the presence of a functional *DGT* allele (Fig. S3).

Histochemical analysis of *DR5* promoter activity revealed no discernible staining difference in both *SP* and *sp* seedlings incubated in water, although roots of the *sp* mutant

showed a shorter trace of GUS precipitate in the vascular cylinder (Fig. 5). Exogenous IAA, however, strongly induced GUS expression in *SP* compared to *sp* plants, which was evident both in seedlings and in root tips and confirmed by fluorimetric GUS quantitation (Fig. 5). Fainter GUS staining was observed for both auxin treated and untreated roots in the *dgt* mutant (Fig S4). As PIN-FORMED (PIN) auxin efflux transporters are key players determining auxin distribution in plants, we quantified the relative expression of the *PIN1*, *PIN2* and *PIN3* genes in roots with or without prior auxin incubation. Auxin treatment induced *PIN1* and *PIN3* expression in all genotypes, except in the *sp dgt* double mutant (Fig. 5). *PIN2* expression was reduced by auxin incubation in *SP DGT*, *SP dgt* and *sp dgt*, but not in *sp DGT* (*i.e.* cv Micro-Tom), where a low basal level of expression was observed for all three genes.

Finally, we determined whether auxin affects *SP* at the transcriptional level, as suggested by the presence of auxin-response elements (TGTCTC, and their degenerate version, TGTCNC) (Ulmasov et al., 1995) in the 3´ and 5´ flanking regions of the *SP* gene in tomato and related Solanaceae species (Fig. 6). Analyzing *SP* mRNA levels in seedlings of *SP DGT* and *sp DGT* plants sprayed with IAA or a mock solution, revealed that *SP* expression was induced by IAA treatment in both genotypes. Importantly, *SP* transcript levels were significantly higher in *dgt* mutant plants both in IAA-treated and control seedlings (Fig. 6). We further assessed the effect of *SP* and *DGT* on the mRNA levels of the key players in the auxin signaling cascades, including some members of the *AUXIN RESPONSE FACTORS* (*ARF*) and *AUXIN/INDOLE-3-ACETIC ACID INDUCIBLE* (*Aux/IAA*) gene families, which were chosen by their high auxin-inducibility (Audran-Delalande et al., 2012). *SP* and *DGT* had combinatorial effects in the expression levels of *IAA1*, *IAA2*, *IAA9*, *ARF8*, and *ARF10*, whereas functional *DGT* decreased expression of *IAA3* (Fig. 6).

Discussion

Impact of SP alleles, and their interaction with auxin, in the control of shoot architecture

Although it has been previously demonstrated that the *sp* mutation does not alter tomato flowering time or the number of leaves before termination of the shoot (Pnueli et al., 1998; Shalit et al., 2009), *SP* orthologs vary in this respect depending on the species. Flowering time is not affected in *cen* mutants in Antirrhinum (Bradley et al., 1996), whereas Arabidopsis *tfl1* mutants flower earlier and *TFL1* overexpression delays flowering by preventing the meristem transition from vegetative to floral (Ratcliffe et al., 1998). In soybean, where large intraspecific variation exists in time to flowering, association mapping has recently linked this important agronomic trait to the *Dt1* locus, a *CEN*/*TFL1*/*SP* ortholog (Zhang et al., 2015). Comparison of determinate and indeterminate near-isogenic soybean lines consistently showed earlier flowering in the former across different locations and planting seasons (Ouattara and Weaver, 1994). Our data show that loss of *SP* function (*sp* allele) leads to slightly but consistently earlier flowering in tomato, measured either in days after germination or the reduction of the number of nodes before the first inflorescence. Using a near isogenic line harbouring the wild type *Dwarf* (*D*) allele, which codes for a brassinosteroid (BR) biosynthesis gene (Marti et al., 2006), we showed here that this effect is not related to reduced BR levels in MT. This is in agreement with the fact that the phenotypes of the *sp* and *dgt* individual mutants in the MT background closely resemble those published for the same mutations in other tomato cultivars (Carvalho et al., 2011). It is therefore unlikely that the combination of both mutations (*sp* and *dgt*) would be affected epistatically by the *d* allele (Campos et al., 2010). Interestingly, the *dgt* mutation delays the number of days to flowering in either *SP* or *sp* backgrounds (Balbi and Lomax, 2003), apparently by reducing the expression of *SINGLE FLOWER TRUSS* (*SFT*) gene, which encodes the florigen (Evans, 1971; Shalit et al., 2009). It does not, however, significantly affect the number of leaves produced before termination, which is a proven effect of *SFT* and its orthologs in tomato and other species (Kojima et al., 2002; Lifschitz and Eshed, 2006; Navarro et al., 2015). Hence, the loss-of-function *sft* mutant produced 130% more leaves on the primary shoot than the control MT (Vicente e al., 2015). Conversely, transgenic tomato plants overexpressing *SFT* flower after only three or four leaves (Molinero-Rosales et al, 2004; Shalit et al, 2009).

Axillary branching was increased in *sp* mutants in both *DGT* and *dgt* allele backgrounds. The expression of *SP* is higher in axillary meristems, suggesting a possible

role for *SP* in the control of apical dominance (Thouet et al., 2008). Our results reinforce this notion, as *sp* mutants are more profusely branched than wild-type plants. This also agrees with the effects of the *SP* ortholog *Dt1* in soybean, where comparison of determinate and indeterminate isogenic lines revealed an increased propensity to side branching in the former (Gai et al., 1984). The *dgt* mutant responds to auxin treatment of decapitated shoots, which inhibits bud outgrowth to the same extent as in wild-type plants (Cline, 1994). Apical dominance has been reported to be reduced in intact *dgt* plants (Coenen et al., 2003), but caution should be exercised when interpreting these results, as published work on *dgt* has been conducted in tomato cultivars differing in their *SP* alleles (Supplementary Table 1). Our results indicate a strong and complex interaction between *SP* and *DGT* in the control of apical dominance: the *dgt* mutation increased it in the wild-type *SP* background, but also increased axillary bud outgrowth in the *sp* background, enhancing its branching phenotype.

Control of endogenous auxin levels and polar auxin transport by SP and DGT

Endogenous IAA concentration and distribution within tissues determine a wide range of plant developmental processes, including apical dominance, stem growth, vascular patterning, root development and others (Petrášek and Friml, 2009; Ljung, 2013). IAA synthesis is maximal in younger, developing parts of the plant such as leaflets and root apices (Ljung et al., 2002). IAA levels in dark-grown seedlings (Fujino et al. 1988) and roots (Muday et al., 1995) of *sp dgt* and *SP DGT* plants are indistinguishable. However, free IAA levels in aerial parts of seven-day-old light-grown seedlins of *sp dgt* plants were twice as high as in *SP DGT* plants (Fig. 2), suggesting a light-dependent, synergistic influence of the *sp* and *dgt* alleles on auxin synthesis, degradation, or transport.

The above results could reflect changes in IAA biosynthesis, degradation or transport. The reduction in PAT produced by the *dgt* mutation was described previously (Ivanchenko et al., 2015), but the synergistic effect of the *sp* mutation described here was unexpected. The differences in IAA concentration in the aerial part of the seedlings could be due to altered PAT caused by both the *sp* and *dgt* mutations. PAT from the shoot organs to the root tips induces the formation of the entire plant vascular system (Aloni, 2013; Marcos and Berleth, 2014), as evidenced by the repression of protoxylem formation upon

treatment with the auxin transport inhibitor NPA (Bishopp et al, 2012) and the polar localization of PIN1 in pre-procambial cells (Scarpella et al, 2006). Lack of large secondary xylem vessels was conspicuous in the *dgt* mutant, as previously described (Zobel, 1974). In plants harbouring the functional *DGT* allele, the effect of the *sp* mutation was to increase the incidence of larger (>800 μm^2 cross-sectional area) vessels. In tree species, there is evidence that the relationship between xylem vessel density and size involves differential regulation of the duration of tracheid expansion along the longitudinal (Anfodillo et al, 2012; Sorce et al, 2013) and radial (Tuominen et al, 1997) axes. Tree stature has a strong influence on vessel width due to an allometric scaling effect (Morris et al, 2017). It remains to be seen if this is also the case in herbs, and if the effect of the *SP* gene on xylem width is indirectly caused by its control of plant height, or directly by its influence on PAT. Increased PAT in the *polycotyledon* tomato mutant, for instance, leads to an altered vascular pattern in the hypocotyl (Al-Hammadi et al, 2003; Kharshiing et al, 2010).

SP affects excised hypocotyl elongation, gravitropic responses, and root regeneration and elongation

Elongation of excised hypocotyl segments in response to different concentrations of exogenous auxin is a classical assay for auxin sensitivity (Gendreau et al., 1997; Collett et al., 2000). The hypocotyl elongation response of *dgt* has been described in the background of tomato cultivar VFN8, a mutant for *sp* (Supplemental Table 1). In both intact or excised hypocotyl segments, a reduced response to exogenous auxin was observed for the *sp dgt* double mutant (Kelly and Bradford, 1986; Rice and Lomax, 2000). We confirmed these results, but show that a functional *SP* allele leads to increased elongation in either *DGT* or *dgt* backgrounds. Collectively, these results indicate that some compensatory effect can be ascribed to SP on this response. Hypocotyl elongation in Arabidopsis relies on auxin-induced changes in the activity of plasma membrane H^+-ATPases, which leads to increased H^+ extrusion and cell expansion, through expansin-mediated cell wall loosening, as per the acid growth theory (Takahashi et al., 2012). Hypocotyl elongation upon exogenous auxin application, points to a positive effect of SP on the activity of plasma membrane H^+-ATPases. Interestingly, the activity of both plasma membrane H^+-ATPases and PIN efflux transporters, which are also influenced by SP at the transcriptional level (Fig. 4), is

328 regulated by changes in their phosphorylation state (Takahashi et al., 2012; Zourelidou et
329 al., 2014; Weller et al., 2017). This fits with earlier suggestions that *SP*, which encodes a
330 phosphatidylethanolamine binding protein (PEBP), exerts at least some of its effects on
331 membrane proteins through interaction with kinases (Pnueli et al., 2001).

332 The Cholodny-Went hypothesis is a classical model suggesting that differential
333 auxin distribution is the cause of directional plant bending with respect to an exogenous
334 stimulus such as light or gravity (Went, 1974). That DGT is required for a correct
335 gravitropic response of roots and shoots has been demonstrated, but the explanation at the
336 molecular level is still lacking (Muday et al., 1995; Rice and Lomax, 2000). To the best of
337 our knowledge, an effect of SP on shoot gravitropism had not been tested before.
338 Functional SP enhances shoot gravitropism in horizontally positioned plants of either *DGT*
339 or *dgt* background. Functional SP produces taller plants, so it is tempting to speculate that
340 they should have a stronger gravitropic response in order to facilitate the bending of a
341 larger stem. In Arabidopsis, the IAA efflux transporter PIN3 mediates lateral redistribution
342 of auxin and is therefore involved in hypocotyl and root tropisms (Friml et al., 2002). It
343 seems reasonable to suggest a link between SP and PIN3 in the face of our *PIN* gene
344 expression profiles (Fig. 5). Remarkably, both types of efflux transporters, PIN1 and PIN3,
345 have been shown to relocate at the subcellular level via the same mechanism: vesicle
346 trafficking along the actin cytoskeleton between the plasma membrane and endosomes
347 (Geldner et al., 2001; Friml et al., 2002). Dissecting the intertwined mechanisms involved
348 in this possible co-regulation will be required to fully understand to which extent and how
349 exactly SP affects auxin distribution.

350 High concentrations of exogenous auxin inhibit root elongation. As expected, the
351 *dgt* mutation reduced auxin-induced inhibition (Coenen and Lomax, 1998) in root
352 elongation, however, a functional *SP* allele led to lower inhibition than in the double *sp dgt*
353 mutant. This result could be ascribed to a new balance in auxin transport and signaling
354 produced by the combination of *SP* and *DGT*. Root growth increases with the strength of
355 auxin signaling up to a certain optimum, and then begins to decline, probably following a
356 parabolic trajectory (Sibout et al, 2006). *In vitro* root regeneration, on the other hand, is
357 stimulated by low concentrations of auxin and *dgt* is relatively insensitive to this exogenous

358 treatment (Coenen and Lomax, 1998). Interestingly, the *sp* mutation also reduces
359 rhizogenesis (Fig S3), which reinforces the notion of *SP* positively influencing PAT, as the
360 PAT inhibitor TIBA has been shown to reduce *in vitro* root formation in tomato (Tyburski
361 and Tretyn, 2004).

362 *Interactions between SP and the auxin signaling machinery*

363 Auxin signaling output can be estimated by following *DR5* promoter activation
364 pattern (Ulmasov et al., 1995; Liao et al., 2015). For example, GUS staining of *DR5::GUS*
365 has revealed that auxin flux at the root tips proceeds acropetally up to the root cap, where it
366 is redistributed via lateral efflux transporters toward a peripheral basipetal transport route
367 (Benková et al., 2003; Paciorek et al., 2005; Dhonukshe et al., 2008). Exogenous auxin
368 application leads to greater GUS signal in seedlings with a functional *SP* allele, owing
369 probably to alterations in the auxin signaling machinery produced by SP, such as
370 expression of *Aux*/*IAA* and *ARF* family genes (Fig. 6).

371 Auxin signalling is strongly dependent on auxin levels and the responsiveness of
372 target cells. At low IAA levels, a suite of repressor proteins, including Aux/IAA and
373 TOPLESS, repress ARFs, a group of transcription factors which regulate the expression of
374 auxin-responsive genes (Causier et al., 2012; Bargmann and Estelle, 2014; Chandler, 2016).
375 At high IAA levels, auxin acts as a molecular glue to stabilize the TIR1/AFB receptor
376 binding and tagging of Aux/IAAs for 26S proteasome degradation (Hayashi, 2012). This, in
377 turn, frees ARFs bound to Auxin-Response Elements (AuxRE) in the genome (TGTCTC,
378 or its degenerate, but also functional form, TGTCNC) to activate or repress gene expression
379 (Ulmasov et al., 1995). Our *in silico* analyses demonstrated the presence of conserved
380 AuxRE elements both 5´ (upstream) and 3´ (downstream) of the *SP* coding sequence in the
381 genome of tomato and closely related species. It has recently been shown that the 3´ region
382 of *TFL1* in Arabidopsis contains multiple auxin *cis*-regulatory elements key for the control
383 of spatio-temporal expression of the gene (Serrano-Mislata et al., 2016). It remains to be
384 determined whether such *cis*-regulatory elements are also functional in tomato and if they
385 are involved in the response of *SP* expression to auxin.

386 Tomato has 25 *Aux*/*IAA* and 22 *ARF* genes (Audran-Delalande et al., 2012; Zouine
387 et al., 2014), indicating that auxin signalling is very complex. DGT can alter the expression

of genes related to auxin signaling (Mito and Bennett, 1995), including *Aux/IAA* genes (Nebenführ et al., 2000). It was recently discovered that cyclophilin peptidyl-prolyl isomerases (PPIases) catalyse the *cis*/*trans* isomerisation of peptide bonds preceding proline residues of target peptides, including Aux/IAAs (Jing et al., 2015). Only Aux/IAA peptides of the right conformation can bind to the TIR1 receptor and be tagged for degradation, thus PPIases, such as DGT, are believed to play a key role in auxin perception (Su et al., 2015). It is likely that some transcriptional feedback exists when the right conformers are not produced, as suggested by increased transcript levels of *IAA3* and reduced levels of *IAA9* in *dgt* mutants. Furthermore, our *in silico* analysis shows that the *sp* mutation occurs in a highly conserved *cis*-proline residue in a DPDxPxn10H consensus region in the PEBP domain (Fig. S3), which is a potential target for PPIases. Whether this putative molecular interaction between SP and DGT could account for the phenotypic outcomes shown here, remains to be determined.

Conclusions

Auxin gradients are critical for organogenesis in the shoot apex, however, the influence of this hormone on shoot determinacy, which is a key determinant of growth habit, has never been addressed in depth. Our data provides the first link between auxin and the anti-florigenic protein SELF-PRUNING (SP), the main switch between indeterminate and determinate growth habit in tomato. Although it is not clear whether auxin itself can affect growth habit, a physiological interaction between this hormone and members of the CETS family was clearly demonstrated here. Hence, *SP* alleles affected various auxin-related responses (*e.g*. apical dominance, PIN1-mediated polar auxin transport, vascular differentiation, H^+ extrusion and gravitropism responses), different *SP* orthologs presented AuxREs, and the auxin mutant *dgt* downregulated *SFT* and upregulated *SP* expression. There are now increasing evidences that *SP*/*SFT* genetic module is a hub in crop productivity, affecting heterosis for yield (Krieger *et al.*, 2010) and improving plant architecture and the vegetative-to-reproductive balance (McGarry and Ayre, 2012; Vicente et al., 2015; Zsögön *et al.*, 2017). Our results suggest that at least part of the effect of the

417 SP/SFT module on yield is mediated by auxin. This knowledge may inspire novel and more
418 precise manipulation of this hormone for applications in agriculture.

419

420 **Materials and methods**

421 **Plant material**

422 Seeds of the tomato (*Solanum lycopersicum*, L.) cultivar Micro-Tom (MT) were
423 kindly donated by Dr. Avram Levy (Weizmann Institute of Science, Israel) in 1998 and
424 subsequently maintained (through self-pollination) as a true-to-type cultivar. MT seeds
425 carrying the synthetic auxin-responsive (*DR5*) promoter fused to the reporter gene *uid*
426 (encoding a β-glucuronidase, GUS) were obtained from Dr. José Luiz García-Martínez
427 (Universidad Politécnica de Valencia, Spain). The *diageotropica* (*dgt*) mutation was
428 introgressed into MT from its original background in cv. VFN8 (LA1529), donated by Dr.
429 Roger Chetelat (Tomato Genetics Resource Center, Davis, University of California, USA).
430 The functional allele of *SELF-PRUNING* was introgressed from cv. Moneymaker
431 (LA2706).

432 Introgression of mutations into the MT cultivar was described previously (Carvalho
433 et al., 2011). A comparison between indeterminate (*SP/SP*) and determinate (*sp/sp*) plants
434 in the MT background has been published previously (Vicente et al., 2015). Both *sp* and
435 *dgt* mutations were confirmed by CAPS marker analyses and sequencing, respectively. All
436 experiments were conducted on BC_6F_3 plants or subsequent generations (Sestari et al.,
437 2014). *In vitro* seedling cultivation was conducted under controlled conditions (16h/8 h
438 day/night, approximately 45 µmol m^{-2} s^{-1} PAR, 25±1ºC) in flasks with 30 ml of MS/2
439 media gellified with 0.5% agar, pH 5.8. Seeds were surface sterilized by agitation in 30%
440 (v/v) commercial bleach (2.7% sodium hypochlorite) for 15 min followed by three rinses
441 with sterile distilled water.

442

443 **Growth conditions**

Plants were grown in greenhouse in Viçosa (642 m asl, 20°45' S; 42°51' W), Minas Gerais, Brazil, under semi-controlled conditions: mean temperature of 28°C, 11.5 h/13 h (winter/summer) photoperiod, and 250-350 μmol m^{-2} s^{-1} PAR irradiance and irrigation to field capacity twice a day. Seeds were germinated in 350-mL pots with a 1:1 (v/v) mixture of commercial potting mix Basaplant® (Base Agro, Brazil) and expanded vermiculite supplemented with 1g L^{-1} 10:10:10 NPK and 4 g L^{-1} dolomite limestone ($MgCO_3$ + $CaCO_3$). Upon appearance of the first true leaf, seedlings of each genotype were transplanted to pots containing the soil mix described above, except for the NPK supplementation, which was increased to 8 g L^{-1}.

Auxin quantification

Endogenous indole acetic acid (IAA) levels were determined by gas chromatography tandem mass spectrometry-selecting ion monitoring (GC-MS-SIM, Shimadzu model GCMS-QP2010 SE). Samples (50-100 mg fresh weight, FW) were extracted and methylated as described in (Rigui et al., 2015). About 0.25 μg of the labeled standard [$^{13}C_6$]IAA (Cambridge Isotopes, Inc.) was added to each sample as internal standards. The chromatograph was equipped with a fused-silica capillary column (30m, ID 0.25 mm, 0.50 μm thick internal film) DB-5 MS stationary phase using helium as the carrier gas at a flow rate of 4.5 mL min^{-1} in the following program: 2 min at 100°C, followed a ramp by 10°C min^{-1} to 140°C, 25°C min^{-1} to 160°C, 35°C min^{-1} to 250°C, 20°C min^{-1} to 270°C and 30°C min^{-1} to 300°C. The injector temperature was 250°C and the following MS operating parameters were used: ionization voltage, 70 eV (electron impact ionization); ion source temperature, 230°C; interface temperature, 260°C. Ions with a mass ratio/charge (m/z) of 130 and 189 (corresponding to endogenous IAA) and 136 and 195 (corresponding to [$^{13}C_6$]-IAA) were monitored and endogenous IAA concentrations were calculated based on extracted chromatograms at m/z 130 and 136.

Polar auxin transport analysis

Polar auxin transport (PAT) was assayed in hypocotyl segments of 2-week-old seedlings according to the protocol originally described by (Al-Hammadi et al., 2003) with some modifications. Briefly, 10 mm hypocotyl sections were excised and incubated in 5 mM phosphate buffer (pH 5.8) containing 1 µM IAA for 2 h at 25 ± 2°C on a rotary shaker (200 rpm). These segments were placed between receiver (1% [w/v] agar in water) and donor blocks (1% [w/v] agar in 5 mM phosphate buffer [pH 5.8] containing 1 µM IAA and 100 nM ^{3}H-IAA) oriented with their apical ends toward the donor blocks. After 4 h of incubation inside a humid chamber at 25 ± 2°C, the receiver blocks were removed and stored in 3 mL scintillation cocktail (Ultima Gold™, PerkinElmer, USA). Receiver blocks plus scintillation cocktail were shaken overnight at 100 rpm and 28 ± 2°C before analysis in a scintillation counter. As negative control, some hypocotyl segments were sandwiched for 30 min between 1-*N*-natphthylphthalamic acid (NPA)-containing blocks (1% [w/v] agar in water containing 20 µM NPA) prior the auxin transport assays. ^{3}H d.p.m. was converted to fmol auxin transported as described in (Lewis and Muday, 2009).

Auxin sensitivity assays

Root regeneration from cotyledon explants was conducted as described (Cary et al, 2001). Briefly, cotyledon explants were obtained from eight-day old seedlings germinated *in vitro* in half-strength MS medium. The explants were then incubated on Petri dishes containing MS with or without supplementation with 0.4 µM NAA. After 8 days, the number of explants with visible roots (determined using a magnifying glass) was counted.

For hypocotyl elongation assays, hypocotyls were excised from two week-old seedlings and cut into 5-mm sections. Between 15 and 20 segments were pre-incubated for each treatment, floated on buffer (10 mM KCl, 1 mM MES-KOH [pH 6.0], and 1%[w/v] Suc for 2 h at 25ºC in the dark to deplete endogenous auxin. Segments were then incubated on buffer (10 mM KCl, 1 mM MES-KOH [pH 6.0], and 1%[w/v] Suc and NAA at the indicated concentration for 24 h on a shaker at 25ºC under white light. Segments were photographed to determine their length using ImageJ (NIH, Bethesda, MA, USA). The experiment was repeated three times with similar results.

For the gravitropism assays, plants were germinated in 350 ml pots and transferred to 50 mL Falcon tubes two days afer germination (dag). The gravitropic response was assessed 10 dag by placing five plants of each genotype horizontally and photographing them in 30 minute intervals. The angle of shoot bending at each time point was determined using AutoCad 2016 (Autodesk, Inc., San Rafael, CA, Estados Unidos da América). Sterilized seeds were germinated in petri dishes onto two layers of filter paper moistened with distilled water, and incubated for 4 d at 25ºC in the dark. Ten germinated seeds with radicles of 5-10 mm were transferred to vertically oriented square Petri dishes (120 mm × 120 mm) aligned on each plate with the radicles pointing down. The plates contained MS medium supplemented with vitamins, pH 5.7, 3% (w/v) sucrose, 0.8% (w/v) agar and 10 μM α-naphthaleneacetic (NAA) for the auxin treatment. Plates were incubated in a growth chamber in the dark.

In vitro root elongation in response to exogenous auxin was assessed as follows. Seeds were surface-sterilized and imbibed for two days at 4°C in the dark on agar plates containing half-strength MS growth medium (Murashige and Skoog, 1962), transferred to growth chamber under control conditions (12h photoperiod, 150 μmol m^{-2} s^{-1} white light, 22°C/20°C throughout the day/night cycle, 60% relative humidity). After four days, ten seedlings per plate were transferred to half-strength MS medium with or without 10μM NAA (α - naphthalene acetic acid - Sigma-Aldrich, St. Louis, MO, USA) and covered completely with aluminum foil for eight days. Root elongation was assessed every second day under dim light conditions.

Histochemical assays

Transgenic *DR5::GUS* plants were incubated overnight at 37°C in GUS staining solution (100 mM NaH_2PO_4; 10 mM EDTA, 0,5 mM $K_4Fe(CN)_6$; 0,05% Triton X-100, 1mM 5-bromo-4-chloro-3-indolyl-beta-D-glucuronic acid). Following GUS staining, samples were washed in a graded ethanol series to remove chlorophyll. Samples were then photographed using a Leica S8AP0 (Wetzlar, Germany) magnifying glass set to 80× magnification, coupled to a Leica DFC295 camera (Wetzlar, Germany). Quantitative GUS

activity was assayed according to Jefferson et al. 1987, with some modifications. Briefly, samples were ground in liquid nitrogen and subsequently homogenized in MUG extraction buffer composed of 50 mM Hepes-KOH (pH 7.0), 5 mM DTT and 0.5% (w/v) PVP. After centrifugation, 200 µL aliquots of the supernatant was mixed with 200 µL GUS assay buffer composed of 50 mM HEPES-KOH (pH 7.0), 5 mM DTT, 10 mM EDTA and 2 mM 4-methylumbelliferyl-β-D-glucuronide (MUG) and incubated at 37 °C for 30 minutes. Subsequently, aliquots of 100 µL were taken from each tube and the reactions were stopped and fluorescence was analyzed using a spectrofluorometer (LS55, Perkin Elmer) with 365 nm excitation and 460 nm emission wavelength (5 nm bandwidth).

Gene expression analyses

Total RNA was extracted from approximately 30 mg FW of sympodial meristems of 10-day old plants following the protocol of the manufacturer (Promega SV total RNA isolation sytem). For auxin treatments plants were previously sprayed with 10 µM IAA or mock-sprayed 24 h prior to RNA extraction. Four biological replicates were used for subsequent cDNA synthesis. Each replicate consisted of a pool of three plants each were used for the analyses, since sympodial meristems are small and did not provide enough biological material for RNA extraction. Two technical replicates were then performed on each of the four samples. RNA integrity was analyzed on 1% agarose gel and RNA concentration was estimated before and after treatment with DNase I (Amplification Grade DNase I, Invitrogen). Total RNA was transcribed into cDNA using the enzyme reverse transcriptases, Universal RiboClone® cDNA Synthesis (Promega, Madison, WI, USA) following the manufacturers' protocols.

For gene expression analyses Power SYBR® green PCR Master Mix was used in MicroAmp™ Optical 96-well reaction plates (both from Applied Biosystems, Singapore) and adhesive film MicroAmp™ Optical (Applied Biosystems, Foster City, CA, USA). The number of reactions from the cycle threshold (CT) as well as the efficiency of reaction were estimated using the Real-Time PCR Miner tool (Zhao and Fernald, 2005).

Relative expression was normalized using actin and ubiquitin; actin was used to calculate ΔΔCT assuming 100% efficiency of amplification of genes (2^- ΔΔCT). Primer

sequences used are shown in Supplementary Table 1. Melting curves were checked for unspecific amplifications and primer dimerization.

In silico sequence analyses

SP gene alignments was performed using the ClustalW alignment option of the Geneious R9 (Biomatters, Auckland, New Zealand) software package.

Statistical analysis

ANOVA and Tukey HSD tests were performed using Assistat 7.6 beta (http://assistat.com). Percentage data were converted to inverse function (1/X) before analysis.

Acknowledgments

This work was supported by funding from the Agency for the Support and Evaluation of Graduate Education (CAPES-Brazil), the National Council for Scientific and Technological Development (CNPq-Brazil), Foundation for Research Assistance of the São Paulo State (FAPESP-Brazil) and the Foundation for Research Assistance of the Minas Gerais State (FAPEMIG-Brazil). We thank CAPES for studentships granted to J.M.R., W.B.S., and D.S.R. FAPESP provided grants for M.H.V. (2016/05566-0), L. F. (2013/18056-2), L.E.P.P. (2015/50220-2), and A.Z. (2013/11541-2). W.L.A. and L.E.P.P. also acknowledge grants from CNPq (grant 307040/2014-3 to L.E.P.P.). We thank Biomatters Ltd. (Auckland, New Zealand) for the kind gift of a Geneious R9 licence.

Table

Table 1. Parameters that define growth habit: (i) number of leaves on the primary shoot (PS) (i.e. number of leaves up to the first inflorescence); (ii) number of leaves on the main shoot (MS) (i.e. number of leaves of PS plus leaves on sympodial units (SU) following the first inflorescence); (iii) height of PS, MS and lateral shoot (LS); iv) internode length (cm); v) leaf angle insertion; vi) diameter of stem and vii) number of flowers, fruits and flowers per inflorescence. Measurements performed 60 days after germiantion. Data are mean ± s.e.m. (n = 10 plants).

	SP, DGT	*SP, dgt*	*sp, DGT*	*sp, dgt*
Number of leaves on the	9.00±0.36 a	9.09±0.28 a	7.50±0.48 b	7.67±0.58 b

primary shoot				
Height of the main shoot	17.45±0.79 a	12.74±0.61 b	13.45±0.49 b	10.70±1.07 b
Length of fourth internode	1.08±0.12 a	1.11±0.07 a	1.28±0.13 a	1.22±0.22 a
Leaf insertion angle	74.81±3.41a	74.87±3.26 a	73.01±4.38 a	63.54±5.22 a
Stem diameter	5.46±0.26 a	4.36±0.12 ab	5.36±0.21 a	4.45±0.1 b
Flowers per inflorescence	7.00±0.71 b	7.80±0.45 a	7.00±0.00 b	7.00±0.5 b
Number of inflorescences	12.4±1.14 a	9.20±1.30 b	7.40±0.89 b	8.80±1.48 b

Different letters indicate statistically significant differences (Tukey's test, $p < 0.05$) among genotypes.

Figure legends

Figure 1. Additive phenotype of the *self-pruning* (*sp*) and *diageotropica* (*dgt*) mutations in tomato cv. Micro-Tom (MT). (A) Representative plants of *SP DGT*; *SP dgt*; *sp DGT* (cv. MT) and *sp dgt*, 90 dag. Note the simultaneous fruit ripening in *sp* compared to *SP*, a well-known effect of the *sp* mutation. The *dgt* mutation delays fruit ripening (at least in part due to its late flowering, as indicated in b) in either genetic background. Bar=10 cm. **(B) Chronological time to flowering in sp and *dgt* mutants.** Percentage of plants (*n*=15) with at least one open flower. MT (*sp DGT*) plants flower earlier than wild type (*SP DGT*), whereas dgt mutants are late flowering. **(C) Developmental time to flowering in *sp* and *dgt* mutants.** The number of leaves produced before the first inflorescence was reduced in *sp DGT* (MT) and increased in genotypes carrying the functional allele of *SP*. Letters indicate statistically significant differences (Dunn's multiple comparisons test $p<0.05$). **(D) *sp* and *dgt* alter expression of the flowering inducer *SINGLE FLOWER TRUSS* (*SFT*).** The *dgt* mutation leads to lower *SFT* expression and thus delays flowering. A minor influence from *SP* reducing *SFT* levels is also noticeable. Asterisks indicate statistically significant differences with the wild-type *SP DGT* (Student's t-test, $p<0.05$). **(E) Effect of *sp* and *dgt* on side branching.** Schematic representation of side branching in shoots of *SP DGT*; *SP dgt*; *sp DGT* (MT) and *sp dgt* (*n*=15). Pie charts depicting the distribution of side branches in each genotype 60 dag. Grey denotes absence of axillary bud; yellow, a visible bud (>1cm) and dark green, a full branch (with one or multiple leaves). Letters indicate statistically significant differences (Dunn's multiple comparisons test $p<0.05$).

Figure 2. Auxin levels in tomato seedlings are affected synergistically by the *self-pruning* (*sp*) and *diageotropica* (*dgt*) mutations. (A) Representative 7-day old seedling showing the dissection points for auxin quantitation. Free IAA levels in (B) leaves + cotyledons, (C) hypocotyls and (D) roots. Data are mean±s.e.m. (*n*=10) Different letters indicate statistically significant differences (Tukey's test, $p<0.05$) among genotypes.

Figure 3. (A) The *self-pruning* (*sp*) mutation exacerbates defective polar auxin transport in hypocotyls caused by *diageotropica* (*dgt*). Basipetal ^{3}H-IAA transport in 10 mm hypocotyl sections of wild-type (*SP*, *DGT*), *SP dgt*, *sp DGT* (cv. Micro-Tom; also the negative control treated with NPA) and double mutant *sp dgt* roots. Data are mean±s.e.m. (*n*=10). Asterisk indicates statistically significant differences between treatments

(ns, non-significant; **p≤0.05; ***p≤0.01, *t*-test). **(B-E) Vascular patterning in *sp* and *dgt* stems**. Cross-sections of the fifth internode taken 45 dag. Bar = 100 µm. **(F) Vessel density and (G) mean vessel size in *sp* and *dgt* stems**. Letters indicate significant differences (p<0.05 ANOVA, Tukey). **(H) Vessel size distribution in the xylem of *sp* and *dgt* mutants**. The x-axis shows the upper values of cross-sectional area for each vessel size category. The bars within each category represent a single individual plant (n=4 per genotype).

Figure 4. Impact of the *self-pruning* (*sp*) mutation on auxin responses in planta. **(A) Kinetics of gravitropic response in the shoot.** Shoot angle after placing plants horizontally at time point 0 (n=5). (**B) Elongation of excised hypocotyls in response to naphthalenacetic acid (NAA).** 6-mm hypocotyl sections were incubated in the indicated NAA concentration for 24 h before measurement. (n=15) **(C-D) Time-course of *in vitro* root elongation of seedlings in control and 10 µM NAA-containing MS medium.** (n=25). In all panels, bars indicate s.e.m. and asterisks indicate statistically significant differences between *SP* and *sp* plants harboring the same *DIAGEOTROPICA* (*DGT*) allele (*p≤0.05; **p≤0.01, *t*-test).

Figure 5. Effects of *SELF-PRUNING* (*SP*) on the auxin signaling and transport machinery *in planta*. (A) Expression pattern of the GUS reporter driven by the auxin-inducible *DR5* promoter. Representative wild-type (*SP*) and mutant (*sp*) seedlings (bar=2 cm) and their root tips (bar=250 µm) in the absence or presence of exogenous auxin (20 µM IAA, 3h) 15 dag. **(B-D) Fluorimetric quantification of GUS precipitate.** Seedlings were sampled 15 dag, after treatment with exogenous auxin (20 µM IAA, 3h) or mock. Values are mean ± s.e.m (n=4). Letters indicate significant differences between genotypes within the same treatment (p<0.05 ANOVA, Tukey). **(E-G) Relative gene expression of *PIN* transporters in roots.** Letters indicate significant differences between genotypes within the same treatment (p<0.05 ANOVA, Tukey)

Figure 6. *SELF-PRUNING* (*SP*) and auxin-signaling gene expression is altered by the *diageotropica* (*dgt*) mutation. (A) Genomic structure of the *SP* gene in solanaceous species: tomato (*S. lycopersicum*), its wild relatives *S. pimpinellifolium* and *S. pennellii* and potato (*S. tuberosum*). The coding sequence is indicated in yellow (exons, thick bars; introns, thin bars). Red blocks indicate the presence of a conserved or degenerate auxin-response element (AuxRE), TGTCNC. **Relative transcript accumulation of *SP* (B) and auxin signaling genes (C) in sympodial meristems.** Tissues were sampled from 10d old plants, 24h after 10 µM IAA or mock spray. Letters indicate significant differences between genotypes within the same treatment (p<0.05 ANOVA, Tukey). Asterisks indicate significant differences with respect to the wild-type *SP DGT* (p<0.05, t-test).

Literature cited

Al-Hammadi ASAA, Sreelakshmi Y, Negi S, Siddiqi I, Sharma R (2003) The

644 polycotyledon mutant of tomato shows enhanced polar auxin transport. Plant Physiol
645 133: 113–125

646 Aloni R (2001) Foliar and axial aspects of vascular differentiation: hypotheses and
647 evidence. J Plant Growth Regul 20: 22-34

648 Aloni R (2013) Role of hormones in controlling vascular differentiation and the mechanism
649 of lateral root initiation. Planta 238: 819–830

650 Alvarez J, Guli CL, Yu X-H, Smyth DR (1992) terminal flower: a gene affecting
651 inflorescence development in Arabidopsis thaliana. Plant J 2: 103–116

652 Anfodillo T, Deslauriers A, Menardi R, Tedoldi L, Petit G, Rossi S (2012) Widening of
653 xylem conduits in a conifer tree depends on the longer time of cell expansion
654 downwards along the stem. J Exp Bot 63:837837a

655 Audran-Delalande C, Bassa C, Mila I, Regad F, Zouine M, Bouzayen M (2012) Genome-
656 wide identification, functional analysis and expression profiling of the Aux/IAA gene
657 family in tomato. Plant Cell Physiol 53: 659–672

658 Balbi V, Lomax TL (2003) Regulation of early tomato fruit development by the
659 *diageotropica* gene. Plant Physiol 131: 186–97

660 Bargmann BOR, Estelle M (2014) Auxin perception: in the IAA of the beholder. Physiol
661 Plant 151: 52–61

662 Bartel B, Fink GR (1995) ILR1, an amidohydrolase that releases active indole-3-acetic acid
663 from conjugates. Science 268: 1745–1748

664 Benková E, Michniewicz M, Sauer M, Teichmann T, Seifertová D, Jürgens G, Friml J
665 (2003) Local, efflux-dependent auxin gradients as a common module for plant organ
666 formation. Cell 115: 591–602

667 Berleth T, Sachs T (2001) Plant morphogenesis: long-distance coordination and local
668 patterning. Curr Opin Plant Biol 4: 57–62

669 Bishop GJ, Nomura T, Yokota T, Harrison K, Noguchi T, Fujioka S, Takatsuto S, Jones
670 JDG, Kamiya Y (1999) The tomato DWARF enzyme catalyses C-6 oxidation in

671 brassinosteroid biosynthesis. Proc Natl Acad Sci U S A 96: 1761–1766

672 Bishopp A, Help H, El-Showk S, Weijers D, Scheres B, et al. (2011) A mutually inhibitory
673 interaction between auxin and cytokinin specifies vascular pattern in roots. Curr Biol
674 21:917–926

675 Blilou I, Xu J, Wildwater M, Willemsen V, Paponov I, Friml J, Heidstra R, Aida M, Palme
676 K, Scheres B (2005) The PIN auxin efflux facilitator network controls growth and
677 patterning in Arabidopsis roots. Nature 433: 39–44

678 Bradley D, Carpenter R, Copsey L, Vincent C, Rothstein S, Coen E (1996) Control of
679 inflorescence architecture in Antirrhinum. Nature 379: 791–797

680 Campos ML, Carvalho RF, Benedito VA, Peres LEP (2010) Small and remarkable. The
681 Micro-Tom model system as a tool to discover novel hormonal functions and
682 interactions. Plant Signal Behav 5: 267-270

683 Carvalho RF, Campos ML, Pino LE, Crestana SL, Zsögön A, Lima JE, Benedito VA, Peres
684 LEP (2011) Convergence of developmental mutants into a single tomato model
685 system: “Micro-Tom” as an effective toolkit for plant development research. Plant
686 Methods 7: 18

687 Cary A, Uttamchandani SJ, Smets R, Van Onckelen HA, Howell SH (2001) Arabidopsis
688 mutants with increased organ regeneration in tissue culture are more competent to
689 respond to hormonal signals. Planta 213: 700–707

690 Causier B, Lloyd J, Stevens L, Davies B (2012) TOPLESS co-repressor interactions and
691 their evolutionary conservation in plants. Plant Signal Behav 7: 325–328

692 Chandler JW (2016) Auxin response factors. Plant Cell Environ 39: 1014–1028

693 Cline MG (1994) The role of hormones in apical dominance. New approaches to an old
694 problem in plant development. Physiol Plant 90: 230–237

695 Coenen C, Christian M, Lüthen H, Lomax TL (2003) Cytokinin inhibits a subset of
696 diageotropica-dependent primary auxin responses in tomato. Plant Physiol 131: 1692–
697 1704

698 Coenen C, Lomax TL (1998) The diageotropica gene differentially affects auxin and
699 cytokinin responses throughout development in tomato. Plant Physiol 117: 63–72

700 Collett CE, Harberd NP, Leyser O (2000) Hormonal interactions in the control of
701 Arabidopsis hypocotyl elongation. Plant Physiol 124: 553–562

702 Dhonukshe P, Tanaka H, Goh T, Ebine K, Mähönen AP, Prasad K, Blilou I, Geldner N, Xu
703 J, Uemura T, et al (2008) Generation of cell polarity in plants links endocytosis, auxin
704 distribution and cell fate decisions. Nature 456: 962–966

705 Domagalska MA, Sarnowska E, Nagy F, Davis SJ (2010) Genetic analyses of interactions
706 among gibberellin, abscisic acid, and brassinosteroids in the control of flowering time
707 in Arabidopsis thaliana. PLoS One 5: e14012

708 Evans LT (1971) Flower induction and the florigen concept. Annu Rev Plant Physiol 22:
709 365–394

710 Friml J (2003) Auxin transport — shaping the plant. Curr Opin Plant Biol 6: 7–12

711 Friml J, Benfey P, Benková E, Bennett M, Berleth T, Geldner N, Grebe M, Heisler M,
712 Hejátko J, Jürgens G, et al (2006) Apical-basal polarity: why plant cells don't stand on
713 their heads. Trends Plant Sci 11: 12–14

714 Friml J, Wiśniewska J, Benková E, Mendgen K, Palme K (2002) Lateral relocation of auxin
715 efflux regulator PIN3 mediates tropism in Arabidopsis. Nature 415: 806–809

716 Fujino DW, Nissen SJ, Jones AD, Burger DW, Bradford KJ (1988) Quantification of
717 indole-3-acetic acid in dark-grown seedlings of the diageotropica and epinastic
718 mutants of tomato (Lycopersicon esculentum Mill.). Plant Physiol 88: 780–784

719 Gai J, Palmer RG, Fehr WR (1984) Bloom and pod set in determinate and indeterminate
720 soybeans grown in China. Agron J 76: 979

721 Gaxiola RA, Palmgren MG, Schumacher K (2007) Plant proton pumps. FEBS Lett 581:
722 2204–2214

723 Geldner N, Friml J, Stierhof Y-D, Jürgens G, Palme K (2001) Auxin transport inhibitors
724 block PIN1 cycling and vesicle trafficking. Nature 413: 425–428

725 Gendreau E, Traas J, Desnos T, Grandjean O, Caboche M, Hofte H (1997) Cellular basis of
726 hypocotyl growth in Arabidopsis thaliana. Plant Physiol 114: 295–305

727 Hayashi K (2012) The interaction and integration of auxin signaling components. Plant Cell
728 Physiol 53: 965–975

729 Hengst U, Albrecht H, Hess D, Monard D (2001) The phosphatidylethanolamine-binding
730 protein is the prototype of a novel family of serine protease inhibitors. J Biol Chem
731 276: 535–540

732 Ivanchenko MG, Zhu J, Wang B, Medvecka E, Du Y, Azzarello E, Mancuso S, Megraw M,
733 Filichkin S, Dubrovsky JG, et al (2015) The cyclophilin A DIAGEOTROPICA gene
734 affects auxin transport in both root and shoot to control lateral root formation.
735 Development 712–721

736 Jefferson RA, Kavanagh TA, Bevan MW (1987) GUS fusions: beta-glucoronidase as a
737 sensitive and versatile gene fusion marker in higher plants. EMBO J. 6: 3901-3907

738 Jing H, Yang X, Zhang J, Liu X, Zheng H, Dong G, Nian J, Feng J, Xia B, Qian Q, et al
739 (2015) Peptidyl-prolyl isomerization targets rice Aux/IAAs for proteasomal
740 degradation during auxin signalling. Nat Commun 6: 7395

741 Kelly MO, Bradford KJ (1986) Insensitivity of the diageotropica tomato mutant to auxin.
742 Plant Physiol 82: 713–717

743 Kharshiing EV, Kumar GP, Ditengou FA, Li X, Palme K, Sharma R (2010) The
744 *polycotyledon* (*pct1-2*) mutant of tomato shows enhanced accumulation of PIN1 auxin
745 transport facilitator protein. Plant Biol 12: 224–228.

746 Kojima S, Takahashi Y, Kobayashi Y, Monna L, Sasaki T, Araki T, Yano M (2002) Hd3a,
747 a rice ortholog of the Arabidopsis FT gene, promotes transition to flowering
748 downstream of Hd1 under short-day conditions. Plant Cell Physiol 43: 1096–1105

749 Krieger U, Lippman ZB, Zamir D (2010) The flowering gene SINGLE FLOWER TRUSS
750 drives heterosis for yield in tomato. Nat Genet 42: 459–463

751 Kroslak T, Koch T, Kahl E, Höllt V (2001) Human phosphatidylethanolamine-binding

protein facilitates heterotrimeric G protein-dependent signaling. J Biol Chem 276: 39772–39778

Kumari S, Roy S, Singh P, Singla-Pareek S, Pareek A (2013) Cyclophilins: Proteins in search of function. Plant Signal Behav 8: e22734

Lavy M, Prigge MJ, Tigyi K, Estelle M, Ashton NW, Cove DJ, Ashton NW, Grimsley NH, Cove DJ, Balbi V, et al (2012) The cyclophilin DIAGEOTROPICA has a conserved role in auxin signaling. Development 139: 1115–1124

Lewis DR, Muday GK (2009) Measurement of auxin transport in Arabidopsis thaliana. Nat Protoc 4: 437–451

Li J, Li Y, Chen S, An L (2010) Involvement of brassinosteroid signals in the floral-induction network of Arabidopsis. J Exp Bot 61: 4221–4230

Liao C-Y, Smet W, Brunoud G, Yoshida S, Vernoux T, Weijers D (2015) Reporters for sensitive and quantitative measurement of auxin response. Nat Methods 12: 207–210

Lifschitz E, Eshed Y (2006) Universal florigenic signals triggered by FT homologues regulate growth and flowering cycles in perennial day-neutral tomato. J Exp Bot 57: 3405–3414

Ljung K (2013) Auxin metabolism and homeostasis during plant development. Development 140: 943-950

Ljung K, Bhalerao RP, Sandberg G (2002) Sites and homeostatic control of auxin biosynthesis in Arabidopsis during vegetative growth. Plant J 28: 465–474

MacArthur JW (1934) Linkage groups in the tomato. J Genet 29: 123–133

Marcos D, Berleth T (2014) Dynamic auxin transport patterns preceding vein formation revealed by live-imaging of Arabidopsis leaf primordia. Front Plant Sci 5: 235

Marti E, Gisbert C, Bishop GJ, Dixon MS, Garcia-Martinez JL (2006) Genetic and physiological characterization of tomato cv. Micro-Tom. J Exp Bot 57: 2037–2047

McGarry RC, Ayre BG (2012) Manipulating plant architecture with members of the CETS gene family. Plant Sci 188–189: 71–81

779 Mito N, Bennett AB (1995) The diageotropica mutation and synthetic auxins differentially
780 affect the expression of auxin-regulated genes in tomato. Plant Physiol 109: 293–297

781 Molinero-Rosales N, Latorre A, Jamilena M, Lozano R (2004) SINGLE FLOWER TRUSS
782 regulates the transition and maintenance of flowering in tomato. Planta 218: 427–434

783 Morita MT (2010) Directional gravity sensing in gravitropism. Annu Rev Plant Biol 61:
784 705–720

785 Morris H, Gillingham MAF, Plavcová L, et al. (2017) Vessel diameter is related to amount
786 and spatial arrangement of axial parenchyma in woody angiosperms. Plant Cell
787 Environ *https://doi.org/10.1111/pce.13091*

788 Muday G, Lomax T, Rayle D (1995) Characterization of the growth and auxin physiology
789 of roots of the tomato mutant, diageotropica. Planta 195: 548–553

790 Murashige T, Skoog F. 1962. A revised medium for rapid growth and bio assays with
791 tobacco tissue cultures. Physiologia plantarum 15, 473:497

792 Navarro C, Cruz-Oró E, Prat S (2015) Conserved function of FLOWERING LOCUS T
793 (FT) homologues as signals for storage organ differentiation. Curr Opin Plant Biol 23:
794 45–53

795 Nebenführ A, White TJ, Lomax TL (2000) The diageotropica mutation alters auxin
796 induction of a subset of the Aux/IAA gene family in tomato. Plant Mol Biol 44: 73–84

797 Oh K, Ivanchenko MG, White TJ, Lomax TL (2006) The diageotropica gene of tomato
798 encodes a cyclophilin: a novel player in auxin signaling. Planta 224: 133–144

799 Ouattara S, Weaver DB (1994) Effect of growth habit on yield and agronomic
800 characteristics of late-planted soybean. Crop Sci 34: 870

801 Paciorek T, Zazímalová E, Ruthardt N, Petrásek J, Stierhof Y-D, Kleine-Vehn J, Morris
802 DA, Emans N, Jürgens G, Geldner N, et al (2005) Auxin inhibits endocytosis and
803 promotes its own efflux from cells. Nature 435: 1251–1256

804 Park SJ, Eshed Y, Lippman ZB (2014) Meristem maturation and inflorescence architecture-

-lessons from the Solanaceae. Curr Opin Plant Biol 17: 70–77

Petrášek J, Friml J (2009) Auxin transport routes in plant development. Development 136:

Pnueli L, Carmel-Goren L, Hareven D, Gutfinger T, Alvarez J, Ganal M, Zamir D, Lifschitz E (1998) The SELF-PRUNING gene of tomato regulates vegetative to reproductive switching of sympodial meristems and is the ortholog of CEN and TFL1. Development 125: 1979–1989

Pnueli L, Gutfinger T, Hareven D, Ben-Naim O, Ron N, Adir N, Lifschitz E (2001) Tomato SP-interacting proteins define a conserved signaling system that regulates shoot architecture and flowering. Plant Cell 13: 2687–2702

Ratcliffe OJ, Amaya I, Vincent CA, Rothstein S, Carpenter R, Coen ES, Bradley DJ (1998) A common mechanism controls the life cycle and architecture of plants. Development 125: 1609-1615

Reinhardt D, Pesce E-R, Stieger P, Mandel T, Baltensperger K, Bennett M, Traas J, Friml J, Kuhlemeier C (2003) Regulation of phyllotaxis by polar auxin transport. Nature 426: 255–260

Repinski SL, Kwak M, Gepts P (2012) The common bean growth habit gene PvTFL1y is a functional homolog of Arabidopsis TFL1. Theor Appl Genet 124: 1539–1547

Rice MS, Lomax TL (2000) The auxin-resistant *diageotropica* mutant of tomato responds to gravity via an auxin-mediated pathway. Planta 210: 906–913

Rick CM (1978) The Tomato. Sci Am 239: 76–87

Rigui AP, Gaspar M, Oliveira VF, Purgatto E, Carvalho MAM de (2015) Endogenous hormone concentrations correlate with fructan metabolism throughout the phenological cycle in *Chrysolaena obovata*. Ann Bot 115: 1163–1175

Rubery PH, Sheldrake AR (1974) Carrier-mediated auxin transport. Planta 118: 101–121

Samach A, Lotan H (2007) The transition to flowering in tomato. Plant Biotechnol 24: 71–82

Scarpella E (2017) The logic of plant vascular patterning. Polarity, continuity and plasticity

in the formation of the veins and of their networks. Curr Opin Genet Dev 45: 34–43

Scarpella E, Marcos D, Friml JJ, Berleth T (2006) Control of leaf vascular patterning by polar auxin transport. Genes Dev 20: 1015–1027

Serrano-Mislata A, Fernández-Nohales P, Doménech MJ, Hanzawa Y, Bradley D, Madueño F (2016) Separate elements of the TERMINAL FLOWER 1 cis-regulatory region integrate pathways to control flowering time and shoot meristem identity. Development 143: 3315-3327

Sestari I, Zsögön A, Rehder GG, Teixeira L de L, Hassimotto NMA, Purgatto E, Benedito VA, Peres LEP (2014) Near-isogenic lines enhancing ascorbic acid, anthocyanin and carotenoid content in tomato (*Solanum lycopersicum* L. cv Micro-Tom) as a tool to produce nutrient-rich fruits. Sci Hortic 175: 111–120

Shalit A, Rozman A, Goldshmidt A, Alvarez JP, Bowman JL, Eshed Y, Lifschitz E (2009) The flowering hormone florigen functions as a general systemic regulator of growth and termination. Proc Natl Acad Sci U S A 106: 8392–8397

Sheldrake AR (1974) The polarity of auxin transport in inverted cuttings. New Phytol 73: 637–642

Sibout R, Sukumar P, Hettiarachchi C, Holm M, Muday GK, Hardtke CS (2006) Opposite root growth phenotypes of hy5 versus hy5 hyh mutants correlate with increased constitutive auxin signaling. PloS Genetics 2:1898-1911

Sorce C, Giovannelli A, Sebastiani L, Anfodillo T (2013) Hormonal signals involved in the regulation of cambial activity, xylogenesis and vessel patterning in trees. Plant Cell Rep 32:885 in

Stevens MA, Rick CM (1986) Genetics and Breeding. *In* J Atherton, J Rudich, eds, tomato Crop a Sci. basis Improv. Chapman & Hall, London, pp 35–100

Su S-H, Gray WM, Masson PH (2015) Auxin: Shape matters. Nat Plants 1: 15097

Takahashi K, Hayashi K -i. K, Kinoshita T (2012) Auxin activates the plasma membrane H+-ATPase by phosphorylation during hypocotyl elongation in Arabidopsis. Plant Physiol 159: 632–641

860 Takahashi N, Hayano T, Suzuki M (1989) Peptidyl-prolyl cis-trans isomerase is the
861 cyclosporin A-binding protein cyclophilin. Nature 337: 473–475

862 Thouet J, Quinet M, Ormenese S, Kinet J-M, Périlleux C (2008) Revisiting the involvement
863 of *SELF-PRUNING* in the sympodial growth of tomato. Plant Physiol 148: 61–64

864 Tian Z, Wang X, Lee R, Li Y, Specht JE, Nelson RL, McClean PE, Qiu L, Ma J (2010)
865 Artificial selection for determinate growth habit in soybean. Proc Natl Acad Sci U S A
866 107: 8563–8568

867 Tuominen H, Puech L, Fink S, Sundberg B (1997) A radial concentration gradient of
868 indole-3-acetic acid is related to secondary xylem development in hybrid aspen. Plant
869 Phys 115: 577-585

870 Tyburski J, Tretyn A (2004) The role of light and polar auxin transport in root regeneration
871 from hypocotyls of tomato seedling cuttings. Plant Growth Regul 42: 39–48

872 Ulmasov T, Liu ZB, Hagen G, Guilfoyle TJ (1995) Composite structure of auxin response
873 elements. Plant Cell 7: 1611–1623

874 Vicente MH, Zsögön A, de Sá AFL, Ribeiro R V., Peres LEP (2015) Semi-determinate
875 growth habit adjusts the vegetative-to-reproductive balance and increases productivity
876 and water-use efficiency in tomato (*Solanum lycopersicum*). J Plant Physiol 177: 11–
877 19

878 Wang Y, Li J (2008) Molecular basis of plant architecture. Annu Rev Plant Biol 59: 253–
879 279

880 Weller B, Zourelidou M, Frank L, Barbosa ICR, Fastner A, Richter S, Jürgens G, Hammes
881 UZ, Schwechheimer C (2017) Dynamic PIN-FORMED auxin efflux carrier
882 phosphorylation at the plasma membrane controls auxin efflux-dependent growth.
883 Proc Natl Acad Sci U S A 114: E887–E896

884 Went FW (1974) Reflections and speculations. Annu Rev Plant Physiol 25: 1–27

885 Wickland DP, Hanzawa Y (2015) The FLOWERING LOCUS T/TERMINAL FLOWER 1
886 gene family: functional evolution and molecular mechanisms. Mol Plant 8: 983–997

887 Yeager AF (1927) Determinate growth in the tomato. J Hered 18: 263–265

888 Zhang J, Song Q, Cregan PB, Nelson RL, Wang X, Wu J, Jiang G-L (2015) Genome-wide
889 association study for flowering time, maturity dates and plant height in early maturing
890 soybean (Glycine max) germplasm. BMC Genomics 16: 217

891 Zhao S, Fernald RD (2005) Comprehensive algorithm for quantitative Real-Time
892 polymerase chain reaction. J Comput Biol 12: 1047–1064

893 Zobel RW (1973) Some physiological characteristics of the ethylene-requiring tomato
894 mutant diageotropica. Plant Physiol 52: 385–389

895 Zobel RW (1974) Control of morphogenesis in the ethylene-requiring tomato mutant,
896 *diageotropica*. Can J Bot 52: 735-741

897 Zouine M, Fu Y, Chateigner-Boutin A-LL, Mila I, Frasse P, Wang H, Audran C, Roustan
898 J-PP, Bouzayen M (2014) Characterization of the tomato ARF gene family uncovers a
899 multi-levels post-transcriptional regulation including alternative splicing. PLoS One 9:
900 e84203

901 Zourelidou M, Absmanner B, Weller B, Barbosa ICR, Willige BC, Fastner A, Streit V, Port
902 SA, Colcombet J, de la Fuente van Bentem S, et al (2014) Auxin efflux by PIN-
903 FORMED proteins is activated by two different protein kinases, D6 PROTEIN
904 KINASE and PINOID. Elife 3: e02860

905 Zsögön A, Cermak T, Voytas D, Peres LEP (2017) Genome editing as a tool to achieve the
906 crop ideotype and de novo domestication of wild relatives: Case study in tomato. Plant
907 Sci 256: 120–130

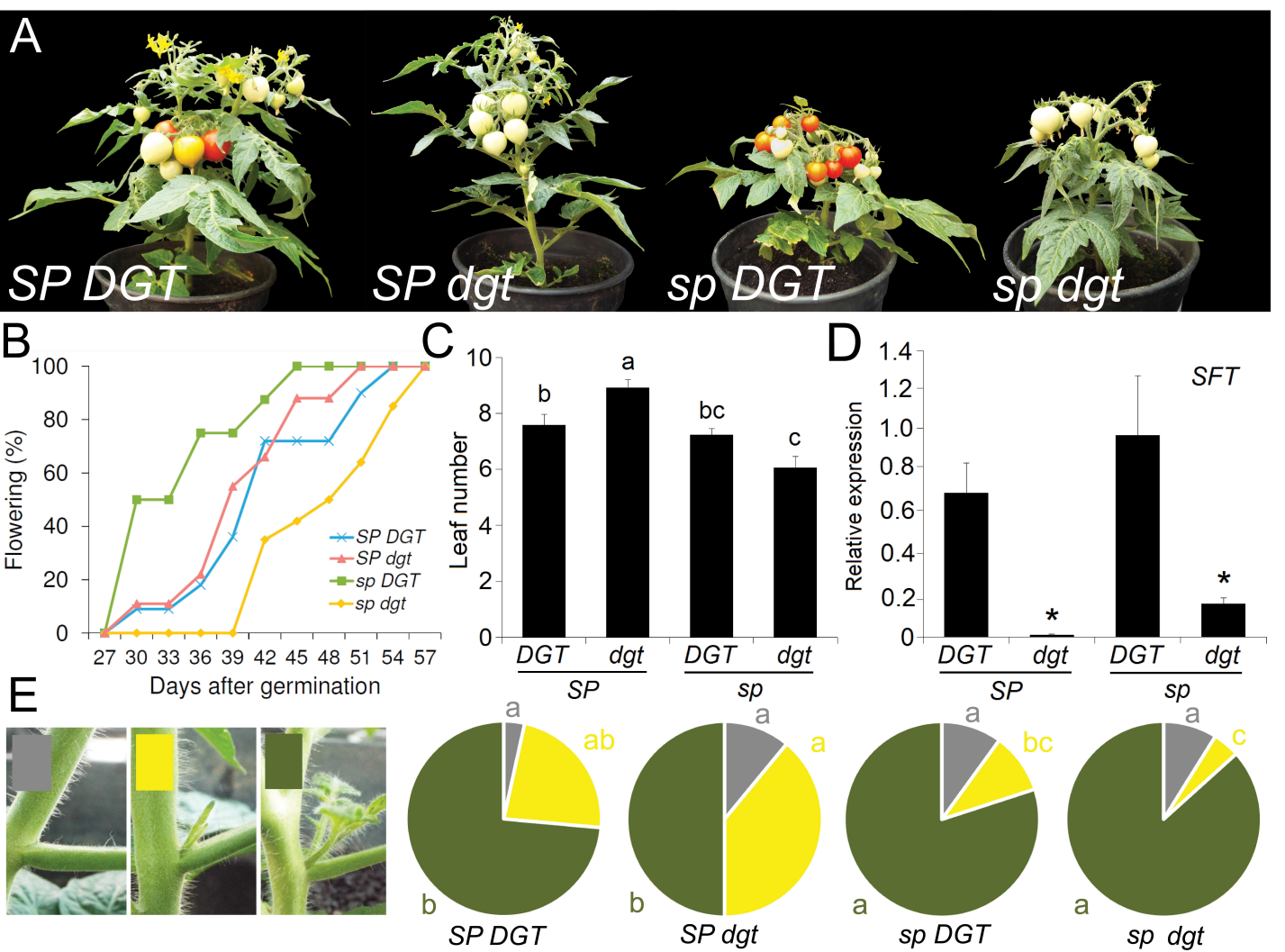
A
SP DGT
SP dgt
sp DGT
sp dgt
B
Flowering (%)
Days after germination
SP DGT
SP dgt
sp DGT
sp dgt
C
Leaf number
DGT
dgt
DGT
dgt
SP
sp
D
SFT
Relative expression
DGT
dgt
DGT
dgt
SP
sp
E
SP DGT
SP dgt
sp DGT
sp dgt

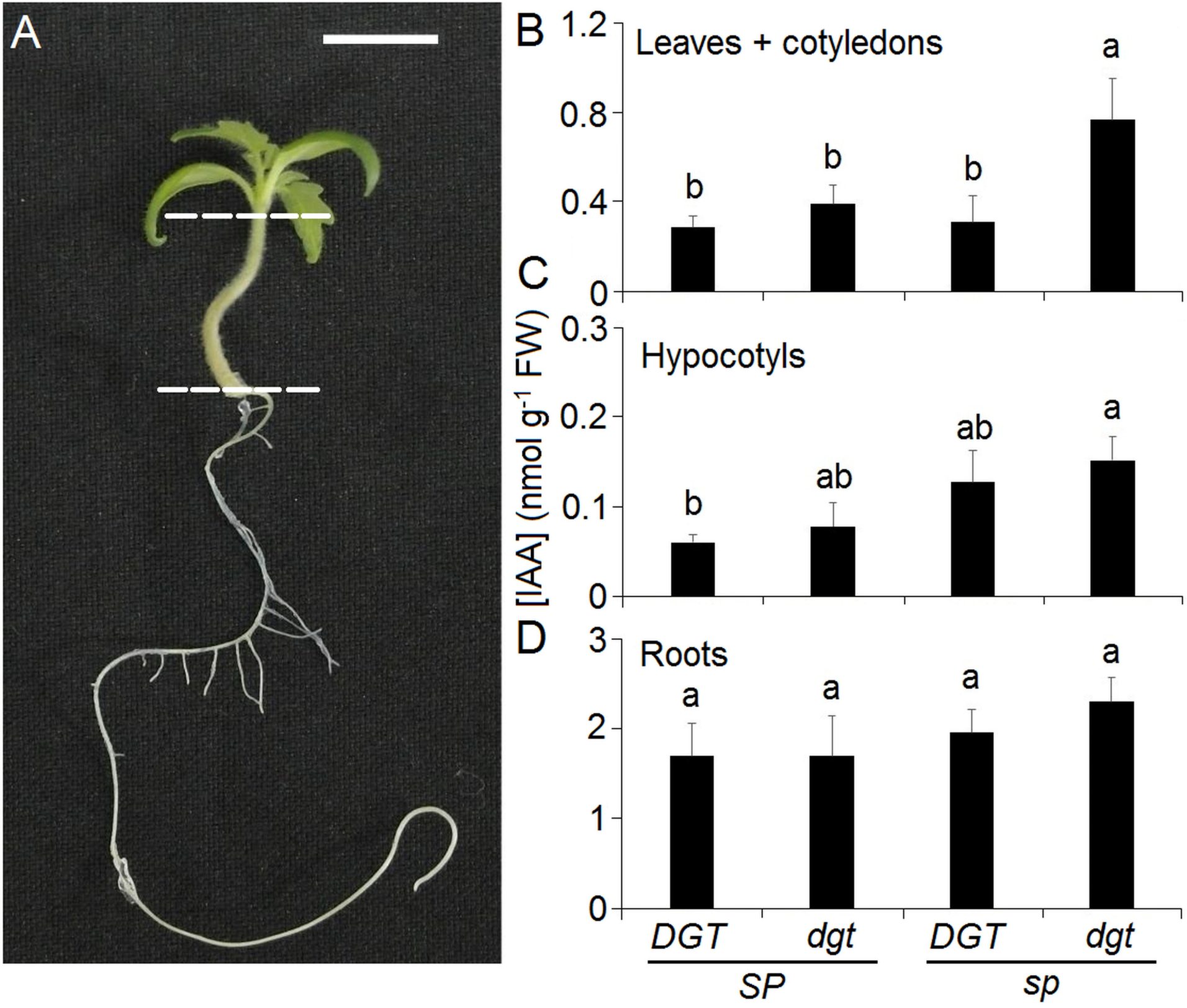
A
B
Leaves + cotyledons
1.2
0.8
0.4
0
b
b
b
a
C
Hypocotyls
0.3
0.2
0.1
0
b
ab
ab
a
[IAA] (nmol g-1 FW)
D
Roots
3
2
1
0
a
a
a
a
DGT
dgt
DGT
dgt
SP
sp

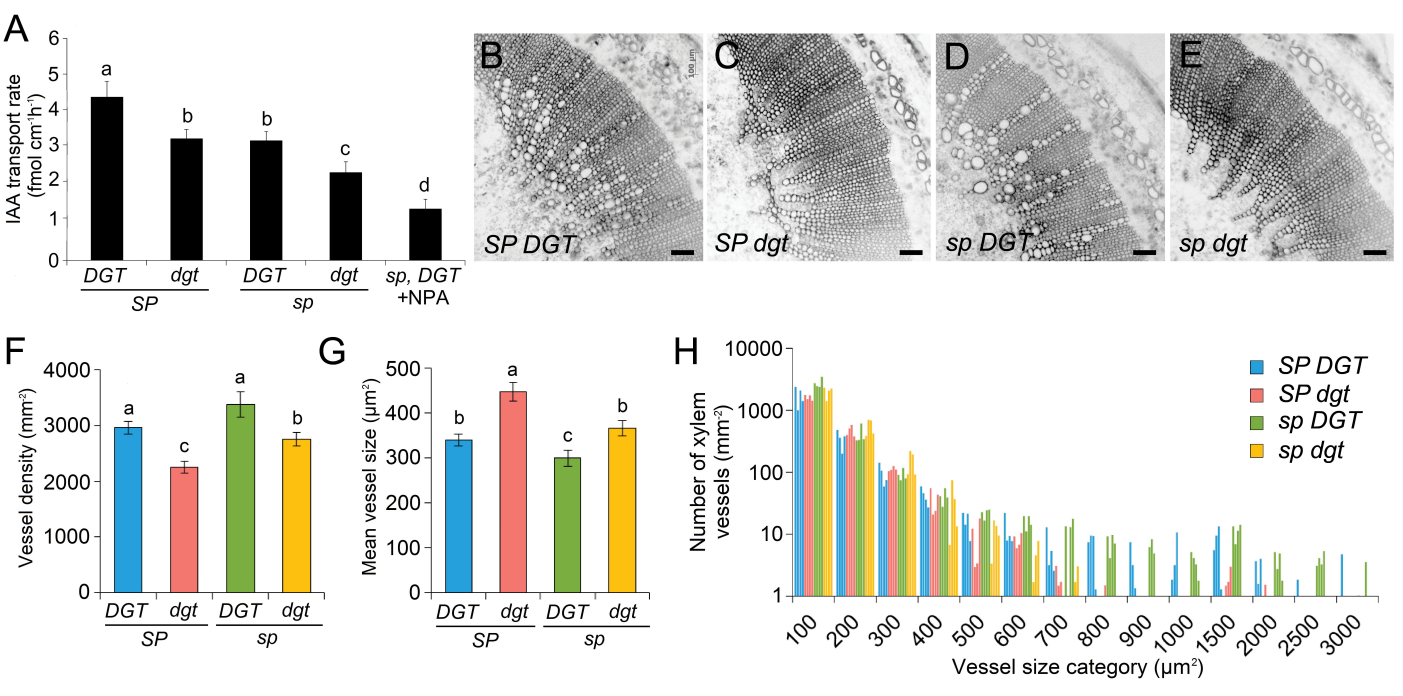
A
IAA transport rate (fmol cm-1h-1)
a
b
b
c
d
DGT
dgt
DGT
dgt
sp, DGT +NPA
SP
sp
B
C
D
E
SP DGT
SP dgt
sp DGT
sp dgt
F
Vessel density (mm2)
G
Mean vessel size (μm2)
H
Number of xylem vessels (mm-2)
SP DGT
SP dgt
sp DGT
sp dgt
Vessel size category (μm2)

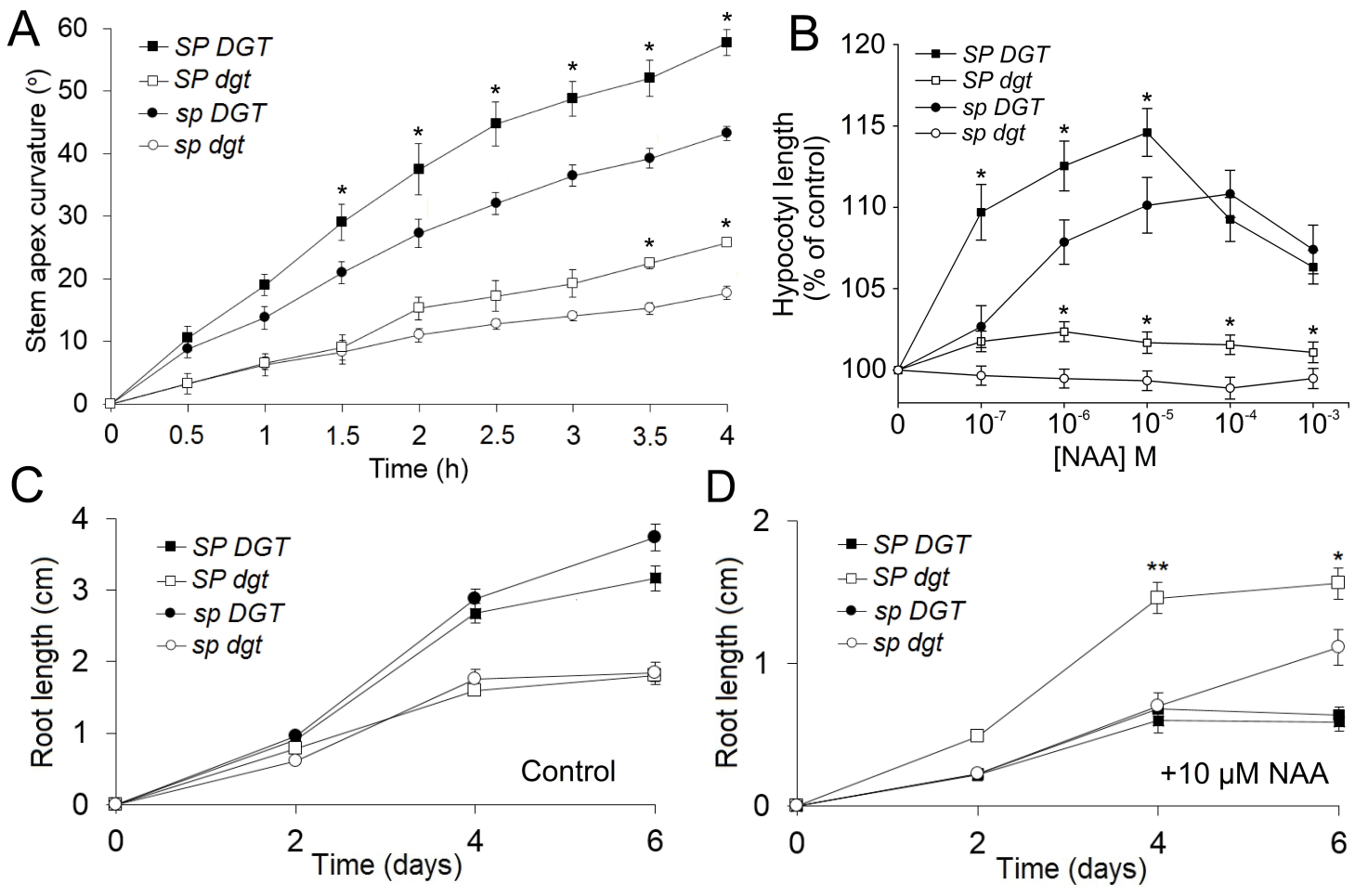
A
Stem apex curvature (°)
Time (h)
SP DGT
SP dgt
sp DGT
sp dgt
B
Hypocotyl length (% of control)
[NAA] M
C
Root length (cm)
Time (days)
Control
D
Root length (cm)
Time (days)
+10 µM NAA

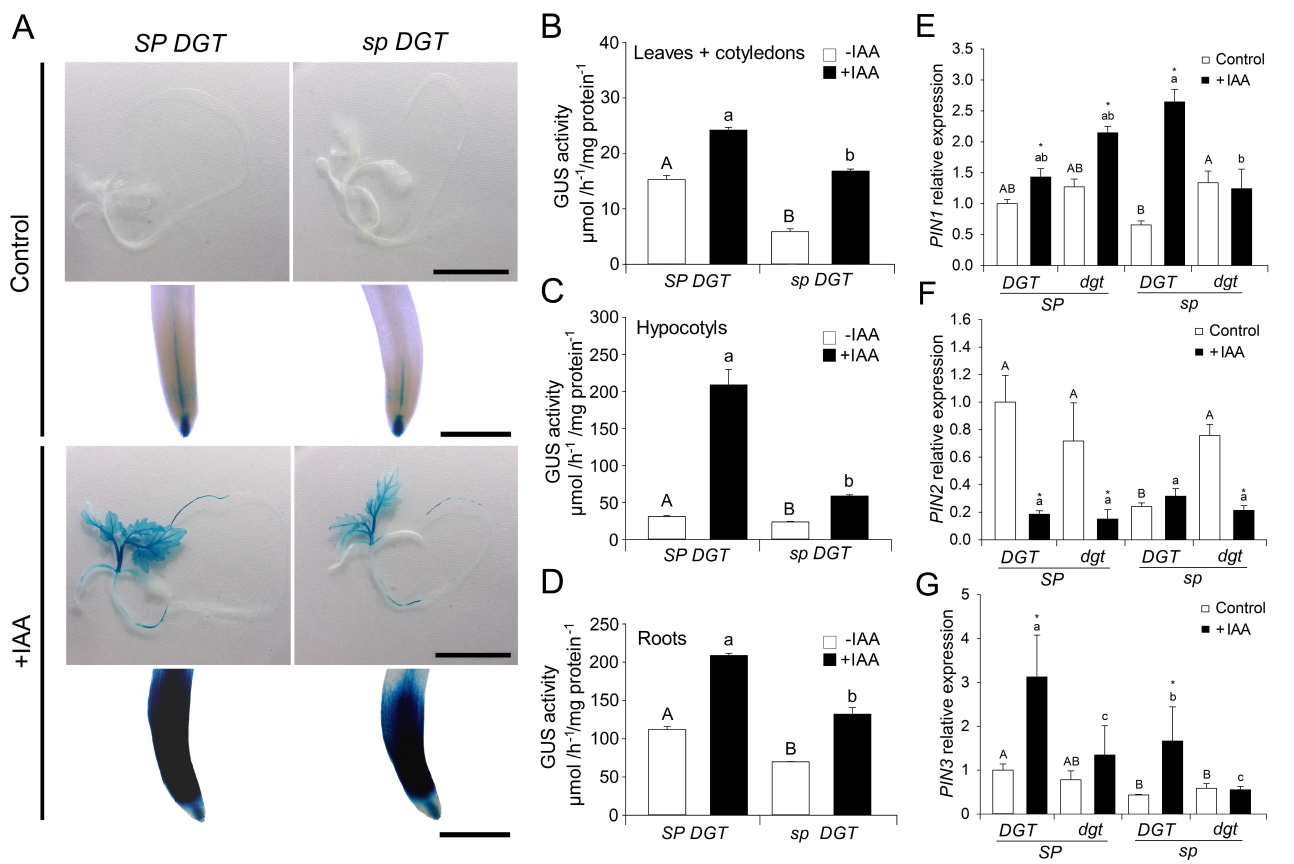
A
SP DGT
sp DGT
Control
+IAA
B
Leaves + cotyledons
-IAA
+IAA
GUS activity
µmol /h-1 /mg protein-1
SP DGT
sp DGT
C
Hypocotyls
D
Roots
E
PIN1 relative expression
Control
DGT
dgt
SP
sp
F
PIN2 relative expression
G
PIN3 relative expression

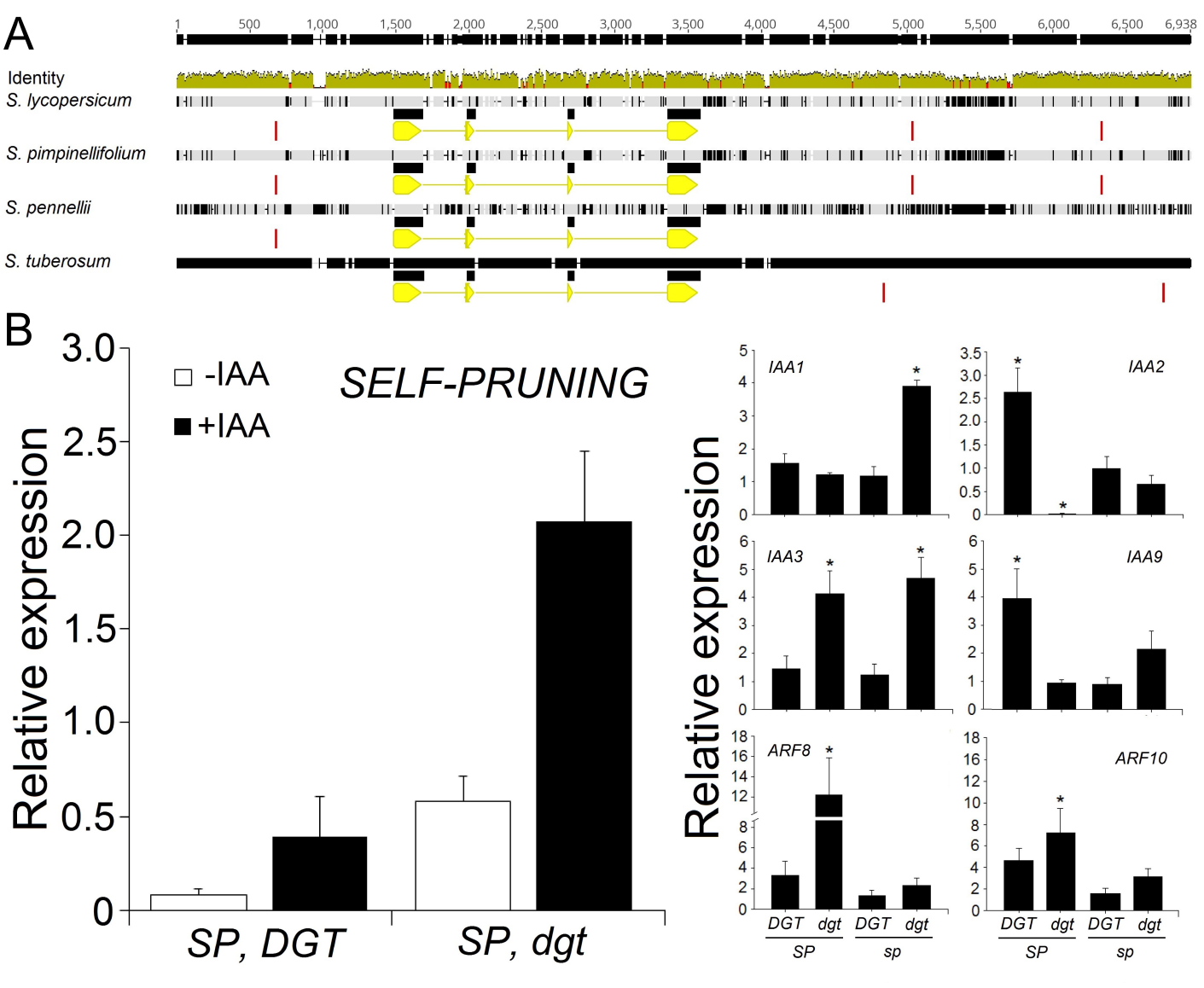
A
1
500
1,000
1,500
2,000
2,500
3,000
3,500
4,000
4,500
5,000
5,500
6,000
6,500
6,938
Identity
S. lycopersicum
S. pimpinellifolium
S. pennellii
S. tuberosum
B
-IAA
+IAA
SELF-PRUNING
Relative expression
3.0
2.5
2.0
1.5
1.0
0.5
0
SP, DGT
SP, dgt
IAA1
IAA2
IAA3
IAA9
ARF8
ARF10
DGT
dgt
SP
sp